tvst
Uveitis

Novel Artificial Intelligence–Based Quantification of Anterior Chamber Inflammation Using Vision Transformers

Carlos Cifuentes-González[1,2,*], Laura Gutiérrez-Sinisterra[1,3,*], William Rojas-Carabali[1,2,4], Joewee Boon[1], Atharva Hudlikar[1], Xin Wei[1], Leonid Shchurov[5], Hnin Hnin Oo[1], Nicholas Chieh Loh[6], Choo Sheriel Shannon[1], Laura Daniela Rodríguez-Camelo[7,8], Bernett Lee[4], Alejandra de-la-Torre[7,8], and Rupesh Agrawal[1–4,6,9]

[1] Department of Ophthalmology, National Healthcare Group Eye Institute, Tan Tock Seng Hospital, Singapore
[2] Programme for Ocular Inflammation & Infection Translational Research (PROTON), Department of Ophthalmology, National Healthcare Group Eye Institute, Tan Tock Seng Hospital, Singapore
[3] Singapore Eye Research Institute, Singapore
[4] Lee Kong Chian School of Medicine, Nanyang Technological University, Singapore
[5] Faculty of Engineering and Information Technology, University of Technology Sydney (UTS), Sydney, Australia
[6] Yong Loo Lin School of Medicine, National University of Singapore, Singapore
[7] Neuroscience (NEUROS) Research Group, Neurovitae Research Center, Institute of Translational Medicine (IMT), Escuela de Medicina y Ciencias de la Salud, Universidad del Rosario, Bogotá, Colombia
[8] Ophthalmology Interest Group, Neuroscience (NEUROS) Research Group, Neurovitae Research Center, Institute of Translational Medicine (IMT), Escuela de Medicina y Ciencias de la Salud, Universidad del Rosario, Bogotá, Colombia
[9] Duke NUS Medical School, Singapore

Correspondence: Rupesh Agrawal, National Healthcare Group Eye Institute, Tan Tock Seng Hospital, Singapore 308433, Singapore.
e-mail: rupeshttsh@gmail.com

Received: October 7, 2024
Accepted: March 22, 2025
Published: May 28, 2025

Keywords: uveitis; optical coherence tomography; artificial intelligence; vision transformer; iris vascularity index, inflammation measurement

Citation: Cifuentes-González C, Gutiérrez-Sinisterra L, Rojas-Carabali W, Boon J, Hudlikar A, Wei X, Shchurov L, Oo HH, Loh NC, Shannon CS, Rodríguez-Camelo LD, Lee B, de-la-Torre A, Agrawal R. Novel artificial intelligence–based quantification of anterior chamber inflammation using vision transformers. Transl Vis Sci Technol. 2025;14(5):31, https://doi.org/10.1167/tvst.14.5.31

Purpose: Quantitative assessment of inflammation is critical for the accurate diagnosis and effective management of uveitis. This study aims to introduce a novel three-dimensional vision transformer approach using anterior segment optical coherence tomography (AS-OCT) to quantify anterior chamber (AC) inflammation in uveitis patients.

Methods: This cross-sectional study was conducted from January 2022 to December 2023 at a single tertiary eye center in Singapore, analyzing 830 AS-OCT B-scans from 180 participants, including uveitis patients at various stages of inflammation and healthy controls. The primary outcomes measured were central corneal thickness (CCT), Iris Vascularity Index (IVI), and Anterior Chamber Particle Index (ACPI). These parameters were assessed using the Swin Transformer V2 artificial intelligence algorithm on AS-OCT images.

Results: The study included 180 participants, including uveitis patients and healthy controls. We observed significant differences between these groups in CCT ($P = 0.01$), ACPI ($P < 0.001$), and IVI ($P < 0.001$). Affected eyes showed elevated CCT and ACPI, along with a significant decrease in IVI, especially in severe inflammation cases. Linear regression analysis underscored a robust correlation between these biometric parameters and inflammation severity in the AC ($R = 0.481$, $P < 0.001$). A 6-month longitudinal study further validated the stability and repeatability of these measurements, affirming their reliability over time.

Conclusions: This study introduces a novel, objective method to quantify ocular inflammation using ACPI, IVI, and CCT, which enhances the precision of assessments over traditional subjective methods prone to interobserver variability. Demonstrated through significant biomarker stability over a 6-month period, our findings support the use of these metrics for reliable long-term monitoring of inflammation progression and treatment efficacy in clinical practice.

Translational Relevance: Our artificial intelligence algorithm objectively quantifies AC inflammation reliably over the time and could be used in the clinic as well as in clinical trials as an objective biomarker.

Introduction

Uveitis is a significant cause of visual impairment, affecting millions worldwide and burdening health care systems substantially.[1] The International Uveitis Study Group classifies uveitis into four types based on the anatomical location of the inflammation: anterior, intermediate, posterior, and panuveitis. Anterior uveitis is the most common form of uveitis in Western countries, characterized primarily by the presence of cells and flare in the anterior chamber (AC).[2]

Despite its clinical significance, the current gold standard for assessing anterior uveitis involves manual estimation of cell count using a slit lamp, a method that is limited by its reliance on the operator's expertise and subjective judgment. This subjectivity leads to significant interobserver variability, even among uveitis specialists. Interobserver agreement for cell counts in the AC is relatively low, with kappa values ranging from 0.34 to 0.43 for cells and from 0.50 to 0.64 for flare.[3]

Recent advancements in ophthalmic imaging and artificial intelligence (AI) have paved the way for more objective and precise methods to assess ocular inflammation. Several models evaluating ocular inflammation in uveitis patients have demonstrated excellent performance, with correlations ranging from 0.74 to 0.94 and precision reaching up to 98%.[4–7] However, these models primarily focus on cellularity in the AC, neglecting other critical aspects of inflammation.

This study introduces and validates a novel three-dimensional (3D) vision transformer approach for quantifying AC inflammation using novel objective parameters such as the Iris Vascularity Index (IVI) and Anterior Chamber Particle Index (ACPI). This study aims to validate an AI-driven approach for quantifying ocular inflammation using central corneal thickness (CCT), ACPI, and IVI as objective biomarkers. Traditional clinical assessments rely on subjective grading, leading to interobserver variability. We hypothesize that these indices correlate with inflammation severity, with higher Standardization of Uveitis Nomenclature (SUN) cell grades associated with increased CCT and ACPI and decreased IVI. We expect CCT to be greater in noninfectious uveitis and IVI to be higher in infectious cases, reflecting distinct inflammatory patterns. Additionally, the ACPI and IVI may vary by uveitis location, with the ACPI being higher in anterior uveitis. Increasing flare severity is anticipated to correlate with higher CCT and ACPI. We also propose that these biomarkers will remain stable over 6 months while responding to disease progression and treatment. By establishing these AI-based metrics, this study aims to improve the precision, reproducibility, and reliability of uveitis assessment, enhancing clinical monitoring and decreasing reliance on subjective grading.

Materials and Methods

Study Design and Recruitment

We conducted a cohort study on patients with uveitis and healthy controls using anterior segment optical coherence tomography (AS-OCT). This study adhered to the STROBE guidelines[8] (Supplementary Material 1) and Consolidated reporting guidelines for prognostic and diagnostic machine learning modeling studies[9] (Supplementary Material 2).

A total of 180 participants were recruited from a single tertiary eye center in Singapore. Both uveitis patients and healthy controls were recruited during the same period. All patients were over 21 years of age and provided informed consent for their participation. Uveitis patients were diagnosed by a uveitis specialist and healthy controls were individuals without a history of uveitis or any ocular disease affecting the aqueous barrier. Healthy controls had only one baseline visit, which included a comprehensive ophthalmic examination and imaging. In contrast, uveitis patients had multiple data points collected over 12 months, with imaging performed at each time point.

Clinical Examination

All participants underwent a comprehensive ocular examination, including best-corrected visual acuity assessment, intraocular pressure measurement, slit-lamp biomicroscopy, and posterior segment evaluation. AC cells and flares were clinically graded using the SUN[10] classification by a uveitis specialist with more than 20 years of experience. Additionally, laboratory tests were conducted to rule out infections and other noninfectious causes of uveitis; cases with no identifiable cause were classified as idiopathic uveitis. Furthermore, all patients were assessed using were assessed AS-OCT (Fig. 1A).

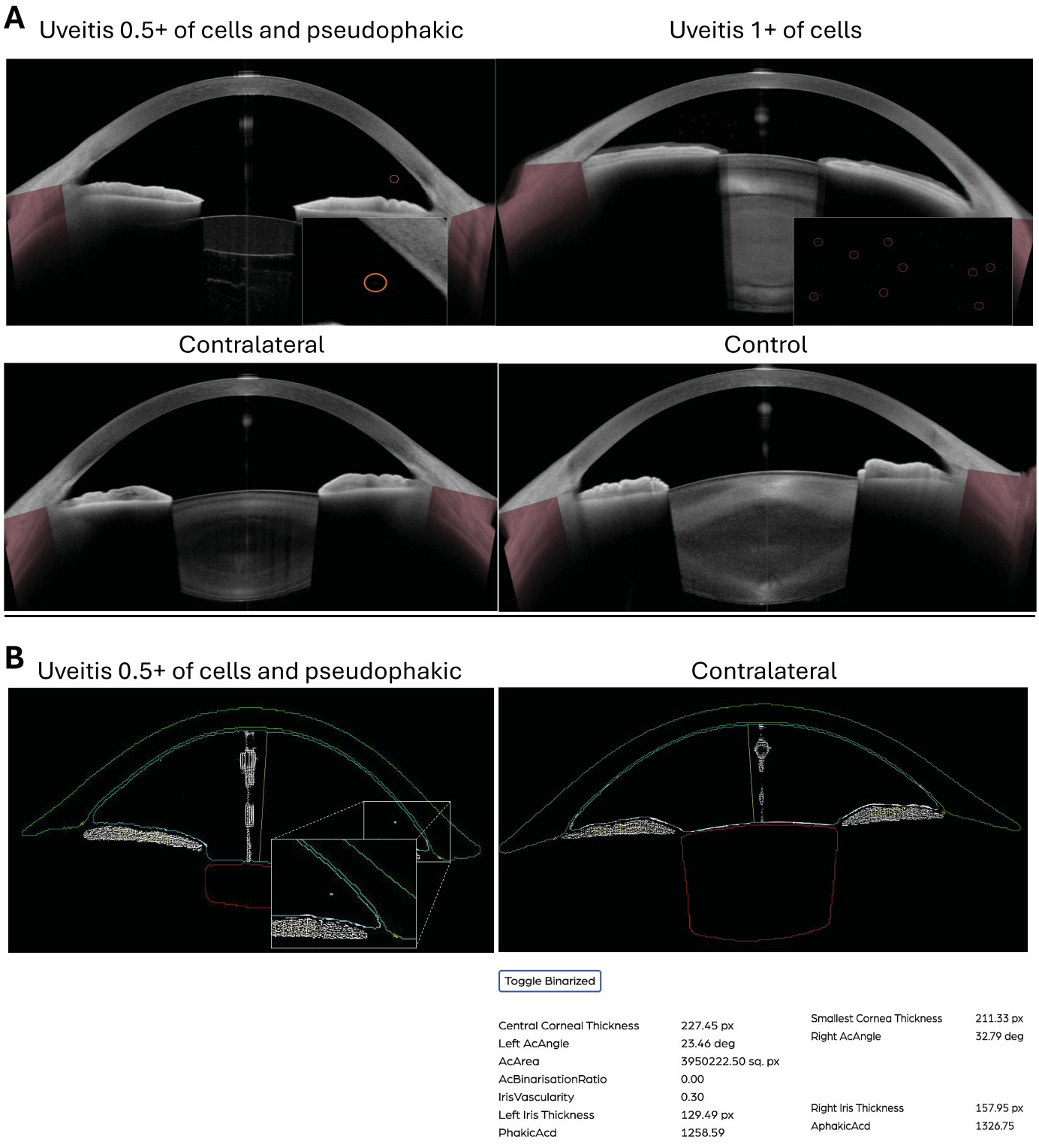

Figure 1. Features of the Images and the Platform Analysis. (**A**) Examples of different types of images from patients with AC inflammation, contralateral eyes of patients with uveitis, and healthy eyes used in this model. (**B**) The different layers automatically generated by the Visual Transformers system and what it segments in patients with AC inflammation.

translational vision science & technology

Data Collection

Clinical data collected included age, sex, ethnicity, cause of uveitis, grade of AC cells, and grade of AC flare at all time points. Eyes were categorized into three groups: (1) healthy, (2) uveitis, and (3) contralateral eyes of unilateral uveitis. Uveitic eyes were further categorized based on the anatomical location of the inflammation according to the SUN classification.

AS-OCT Acquisition Protocol

To assess changes in the anterior segment accurately, we used AS-OCT. Imaging was conducted using a horizontal raster scan pattern centered on the AC. Each session involved acquiring six B-scans to capture comprehensive data across the central zone of the eye. This method was chosen to optimize detail and consistency in imaging while minimizing patient discomfort and variability in data collection across multiple time points. The horizontal raster pattern specifically aids in decreasing test–retest variability, which is crucial for reliable longitudinal analyses of ocular structures.

Development of the AI Algorithm for AS-OCT Image Analysis

For model development, we used a total of 720 images, comprising 200 images retrieved from the internet and 520 images obtained from 130 patients of our cohort. The patient-derived dataset included images from both eyes of individuals, ensuring that no patient contributed more than two different time points to the dataset. In cases where multiple images from the same patient were available, we selected a maximum of two time points, chosen from baseline, 1 month, 3 months, 6 months, or 9 months of follow-up to maintain diversity while preventing overrepresentation. The training population had an average age of 53 ± 15.5 years, with 50% being women. Regarding ethnicity, 58.9% were Chinese, 21.4% were Indian, and 11.1% belonged to other racial backgrounds.

Search Strategy for Internet-Based Images

To collect images from the internet, we conducted systematic searches using open-access repositories and web scraping techniques. Only images with unrestricted access and copyright licenses permitting their distribution, modification, and repurposing were included. These primarily consisted of licenses such as Creative Commons (CC0, CC BY, CC BY-SA) and Public Domain sources. Additionally, images were sourced from blogs, social media platforms, and publicly accessible websites where copyright status was explicitly stated. When copyright information was ambiguous or unspecified, we assumed the images to be free for use owing to their classification in the public domain, adhering to ethical and legal standards. To illustrate the types of images obtained and the segmentation process applied, we provide a sample set of 10 representative images (Supplementary Material 4). However, the full dataset is not shared publicly to preserve privacy and data integrity. Access may be granted upon reasonable request, subject to ethical considerations and data-sharing regulations.

Training and segmentation algorithm: A 384×384 pixels Swin transformer V2 algorithm, as described by Liu et al. (2021),[11] was used for segmentation. The classification heads were replaced with a single deconvolution layer. In the final layer of the model, the logits were multiplied by the exponent of a trainable parameter τ, initialized at 0.07, in line with previously published literature.[12] The logits were also clamped between -100 and 100 to ensure training stability. For the development of our model, we divided the images into three distinct sets: training (618 images), validation (32 images), and testing (70 images). To prevent overfitting, images from the same eye were assigned exclusively to one of these sets, ensuring no overlap and maintaining test result integrity. Additionally, data augmentation techniques were applied, including flipping, zooming, and contrast adjustments, to enhance model robustness. An early stopping protocol was also implemented to halt training when validation loss ceased to decrease, thereby preventing overtraining.

Training involved 100,000 iterations with a batch size of 12 and 4 gradient accumulation steps. The focal Tversky loss function, with $\alpha = 0.5$, $\beta = 0.5$, and $\gamma = 1$ was used with an AdamW optimizer with a learning rate 1e-4 and gradient decay of 1e-5. A cosine scheduler was employed throughout the training process. Augmentation techniques included flipping the image, zooming and cropping, contrast alteration (including using the CLAHE algorithm), and salt and pepper noise.

Algorithm Inference and Evaluation

Inference was performed on images downscaled on the largest axis to 384 pixels while maintaining the aspect ratio. The Sørensen–Dice and intersection over union coefficients were calculated for performance evaluation (Supplementary Material 3).

With the approach described, this new tool allows for pixel measurements of CCT, automatically measuring the central corneal region. For the ACPI, the tool binarizes the image and compares the number of particles detected in the air vs. the AC. Additionally, the IVI

is derived from image binarization, identifying the iris vascular area (IVA) and stromal iris area (SIA). The IVI is calculated by dividing the IVA by the total iris area (IVA + SIA) and multiplying by 100 to obtain the percentage of IVA occupying the iris.

$$IVI = \frac{IVA}{IVA + SIA} x\ 100$$

Model Metrics and Test–Retest Reliability

Our model's accuracy is quantified using Dice score, intersection over union, and precision, consistently demonstrating high reliability with most scores above critical thresholds. Additionally, test-retest analysis confirms the stability of our measurements, showcasing minimal variability across repeated sessions. Detailed findings are available in Supplementary Material 3, underscoring our model's robustness for clinical application.

AS-OCT Imaging Acquisition and Analysis for the Current Study

In this study, all patients underwent imaging using the Anterion device (Heidelberg Engineering, Heidelberg, Germany), a swept-source AS-OCT system. The original scan protocol was used, which operates at a 1300-nm wavelength light source and a speed of 50,000 A-scans/second, to generate comprehensive 3D models of the cornea and anterior segment.[13] The anterior system captures anterior segment images with an axial depth of 14 mm, a lateral width of 16.5 mm, and resolutions of less than 10 µm axially and 30 to 45 µm laterally.[13] Imaging was performed in dark conditions (light intensity, 0.3 lx), with subjects fixating on an internal target (Fig. 1A).

Data were collected from 831 AS-OCTs from all 180 study participants, including eyes from healthy controls, eyes from uveitis patients, and contralateral eyes from the uveitis patients in case the disease is unilateral, generating a total of 4986 AS-OCT B-scan frames. These frames were averaged for each eye to obtain a comprehensive 3D AC measurement of the. Given the absence of established guidelines or recommendations indicating which specific image provides the most information about the structures of the AC, our approach focused on the necessity of a comprehensive analysis of ocular inflammation. This thorough analysis requires evaluating multiple images, as a single image representing a cross-section of the AC might miss inflammatory cells distributed in different parts of the eye, potentially failing to recognize patients with minimal inflammation.

Statistical Analysis

Data analysis was performed using Jamovi statistical software (version 2) (Jamovi, 2021; https://www.jamovi.org/). All graphical representations were produced using R (The R Foundation for Statistical Computing, Vienna, Austria). The primary unit of analysis was the individual eye. Considering the 12-month follow-up period, disease activity was categorized and monitored over time, with particular attention to cases where the disease progressed to bilateral uveitis. Only eyes confirmed to have uveitis in both assessments were included in the analysis. Results are presented as means, standard deviations, and interquartile ranges, reflecting the non-normal distribution of the quantitative variables. Categorical data were expressed in percentages. Normality was tested using the Shapiro–Wilk test, and the Kruskal–Wallis and one-way analysis of variance tests were applied to non-normally and normally distributed data, respectively. Post hoc analyses using Holm's test were conducted to investigate significant differences between groups. Additionally, Spearman's rho correlation and linear regression were used to analyze the relationships and predict cell counts in the AC, was performed assuming no-autocorrelation or multicollinearity among the variables.

Enhanced Evaluations of Biometric Parameters

Further evaluations of the clinical validity of the proposed biometric parameters (ACPI, IVI, and CCT). Receiver operating characteristic curve analyses were performed to establish optimal performance thresholds, maximizing sensitivity and specificity for detecting varying levels of inflammation severity, as classified by flare intensity and AC cell count. The Youden Index was employed to identify the most effective cutoff values, we use R packages pROC, and glmnet. Additionally, multiclass receiver operating characteristic analysis was implemented to distinguish between different inflammation severity levels using a one-vs-rest classification approach.

Longitudinal Analysis on the Changes in Uveitis

Changes in inflammation levels were meticulously assessed. Worsening activity was defined as a two-step increase in the level of inflammation (e.g., AC cells, vitreous haze) or an escalation from grade 3+ to 4+. Conversely, improved activity was identified as a two-step decrease in inflammation or a reduction to grade 0, following the SUN,[10] which is based on clinical reports. All longitudinal comparisons used nonparametric tests for repeated measures using Jamovi.

Ethical Considerations

This study was performed in accordance with the Helsinki Declaration of 1964 and its later amendments. Institutional review board approval was obtained from the National Healthcare Group Domain Specific Review Board (NHG-DSRB), reference number 2020/01182. Informed consent was obtained from all individual participants included in the study. All participants consented to the use of data for research and publication purposes.

Results

Demographics

We studied 180 participants, of whom 50% were female, with an average age of 53.2 ± 14.4 years. Of these participants, 71.7% (n = 129) had uveitis and 28.3% (n = 51) served as controls. Regarding the ethnicity of participants, 57.8% (n = 104) were of Chinese origin, followed by Indian origin (22.2%, n = 40); the remainder account for other or unknown ethnicities. Among the uveitis patients, 58.9% had unilateral uveitis, predominantly anterior (40.3%; 52/129) and posterior (34.9%; 45/129). Most of these patients had infectious etiologies (50.4%), followed by idiopathic uveitis (29.5%). No statistically significant differences were identified when comparing by gender (Table 1).

AS-OCT Analysis

Analysis Based on the Uveitic Eye

In the comparative analysis between patients with uveitis, controls, and contralateral eye we found statistically significant differences in CCT (P = 0.01) and ACPI (P = 0.002) (Supplementary Material 5, Table 1). In the post hoc analysis, CCT was significantly lower in control eyes (P < 0.001) compared with uveitic eyes and the contralateral eyes of the uveitis patients (P = 0.008). For the ACPI, we observed significantly lower values in both control eyes and the contralateral eyes of the uveitis patients compared with uveitic eyes (P = 0.001 and P = 0.027, respectively). Finally, no significant differences were found in IVI among control eyes, uveitic eyes, and their contralateral eyes (Fig. 2A).

Table 1. Demographic Features of All Study Participants

	Females (n = 90)	Males (n = 90)	Total (N = 180)	P Value
Age, years				
Mean ± SD	55 ± 15	51.3 ± 13.6	53.2 ± 14.4	0.17
Participant category (n = 180)				
Control	19 (21.1)	32 (35.6)	51 (28.3)	0.11
Uveitis	71 (78.9)	58 (64.4)	129 (71.7)	
Ethnicity of study participants (n = 180)				
Chinese	53 (58.9)	51 (56.7)	104 (57.8)	0.73
Filipino	2 (2.2)	0 (0)	2 (1.1)	
Indian	17 (18.9)	23 (25.6)	40 (22.2)	
Malay	6 (6.7)	6 (6.7)	12 (6.7)	
Others	12 (13.3)	10 (11.1)	22 (12.2)	
Laterality of uveitis (n = 129)				
Bilateral	29 (40.8)	24 (41.4)	53 (41.1)	0.95
Unilateral	42 (59.2)	34 (58.6)	76 (58.9)	
Anatomical location of uveitis (n = 129)				
Anterior	33 (46.5)	19 (32.8)	52 (40.3)	0.17
Intermediate	2 (2.8)	4 (6.9)	6 (4.7)	
Anterior and intermediate	2 (2.8)	0 (0)	2 (1.6)	
Panuveitis	15 (21.1)	9 (15.5)	24 (18.6)	
Posterior	19 (26.8)	26 (44.8)	45 (34.9)	
Etiology of uveitis (n = 129)				
Idiopathic	27 (38)	11 (19)	38 (29.5)	0.11
Infectious	30 (42.3)	35 (60.3)	65 (50.4)	
Noninfectious	14 (19.7)	12 (20.7)	26 (20.2)	

Results of the χ^2 and Fisher's exact tests, comparing categorical variables between males and females. Values are number (%) unless otherwise noted.

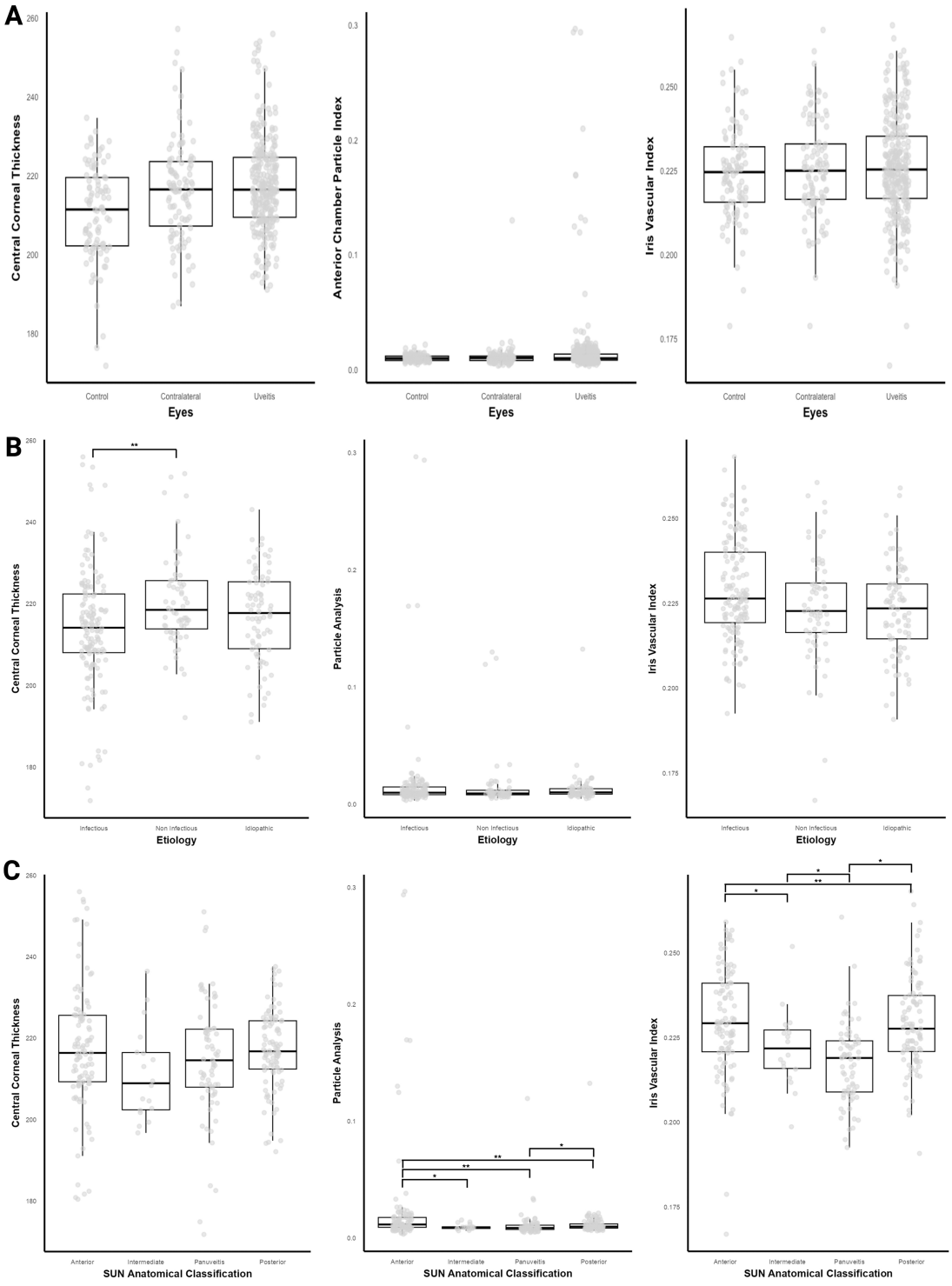

Figure 2. Analysis by eye, etiology, and location of inflammation. Results of the tool's analysis based on one-way analysis of variance or Kruskal–Wallis tests and post hoc tests adjusted by Holm's test for the comparison of numerical variables, with the selection of the test depending on the data distribution. (**A**) Differences found when analyzing CCT, ACPI, and IVI, with results divided into eyes with uveitis, contralateral eyes of patients with uveitis, and healthy control eyes. (**B**) Results of the same measurements in the AC for patients with uveitis, categorized by infectious, noninfectious, and idiopathic etiologies. (**C**) Distribution of the data for the same measurements, but for patients with uveitis divided by the anatomical location of the inflammation (anterior, intermediate, posterior, and panuveitis). Significant differences are highlighted with asterisks (*$P < 0.05$, **$P < 0.01$, ***$P < 0.001$).

Analysis Based on the Etiology of Uveitis

Significant differences were identified in CCT ($P = 0.005$) and IVI ($P = 0.017$) (Supplementary Material 5, Table 2). This subgroup analysis found that the eyes of patients with noninfectious uveitis exhibited greater CCT compared with those with infectious uveitis ($P = 0.002$). Eyes with infectious uveitis were associated with a higher IVI ($P = 0.007$) compared with those with idiopathic uveitis (Fig. 2B).

Analysis Based on the Location of Uveitis

Eyes with anterior uveitis showed higher ACPI values compared with eyes with intermediate uveitis ($P = 0.022$), posterior uveitis ($P < 0.001$), and panuveitis ($P = 0.019$) (Supplementary Material 5, Table 3). Similarly, the ACPI was higher in eyes with panuveitis compared with those with posterior uveitis ($P = 0.037$) (see Fig. 2C). Eyes with anterior uveitis exhibited a higher IVI compared with intermediate and panuveitis ($P = 0.031$ and $P < 0.001$, respectively), and a similar pattern was observed with posterior uveitis compared with intermediate and panuveitis ($P = 0.043$ and $P < 0.001$, respectively) (Fig. 1C).

SUN Cell Grading

Significant statistical associations were observed in all parameters for SUN cell grading and the novel measurement tools evaluated in our study (CCT: $P < 0.001$; ACPI: $P < 0.001$; IVI: $P = 0.03$) (Supplementary Material 5, Table 4). In post hoc analysis, higher CCT values were found in patients with 3+ and 4+ cells compared with eyes with 0+ cells ($P < 0.001$), 0.5+ cells ($P = 0.004$), and 1+ cells ($P = 0.002$) (Fig. 3A). Similarly, CCT was increased in eyes with 2+ cells compared with eyes with 0+ cells (CCT: $P = 0.007$) (Fig. 2A and Supplementary Material 5, Table 4). Regarding ACPI, higher values in the group of patients with 3+ and 4+ cells compared with eyes with 0+ cells ($P < 0.001$), 0.5+ cells ($P = 0.008$), 1+ cells ($P < 0.001$), and 2+ cells ($P = 0.008$). Similarly, patients with 1+ cells had significantly higher ACPI compared with those with 0.5+ cells ($P = 0.047$) and 0+ cells ($P = 0.01$) (Fig. 3A and Supplementary Material 5, Table 4). In contrast with ACPI and CCT, in IVI, patients with 0.5+ cells had a higher IVI than those with 2+ cells ($P = 0.048$) and 3+ to 4+ cells ($P = 0.038$) (Fig. 3A; Supplementary Material 5, Table 4).

Based on the linear regression model, CCT, ACPI, and IVI were found to significantly predict cellularity in the AC, with an R-value close to 0.5 ($P < 0.001$). It was observed that, for each gradient increase in AC cellularity, there is an incremental change of 0.0096 pixels in CCT (($P = 0.002$), 7.62 pixels in ACPI ($P < 0.001$), and a reduction of 6.18% in IVI ($P = 0.025$). For more details, see Table 2.

SUN Flare Grading

We found a difference between different grades of flare and the CCT and ACPI (CCT, $P = 0.038$; ACPI, $P < 0.001$) (Supplementary Material 5, Table 5). In the post hoc analysis of grades of flare, eyes with 1+ flare showed greater CCT than those with 0+ flare (CCT, $P = 0.014$) (Fig. 3B). Additionally, eyes with 1+ flare, and either 2+ or 3+ flare, had a higher ACPI compared with those without flare ($P < 0.001$ and $P = 0.024$, respectively) (Fig. 3B).

Correlations Between the ACPI, CCT, and IVI

IVI exhibited a weak but significant correlation with ACPI ($P = 0.01$). Meanwhile, the CCT had a positive correlation with ACPI ($P < 0.001$), and no correlation was found between the CCT and the IVI (Fig. 3C).

Longitudinal Analyses

In our longitudinal study, we followed 34 patients from baseline to 6 months. Across all participants, we observed a slight decrease in corneal thickness, from an average of 216.522 pixels at baseline to 214.699 pixels at 6 months, although this change was not statistically significant ($P = 0.267$). The ACPI and IVI remained stable throughout the study period, indicating consistent measurement reliability over time. (For more details, see Supplementary Material 6, Figs. A–C.)

In contrast, the subgroup that showed improvement exhibited a significant reduction in corneal thickness, from an average of 217.833 pixels to 212.891 pixels, with a P value of 0.007. This subgroup also experienced a notable decrease in the ACPI, with a mean difference of -0.001 ($P = 0.030$). However, no significant changes were observed in the IVI among the responders (For additional details, see Supplementary Material 6, Figs. D–F).

Performance of the for Different Outputs From AS-OCT

Cell-Grading Inflammation Detection

When distinguishing 2–4+ cell from no cells, CCT was highly effective with an area under the curve (AUC) of 0.78. The cutoff used was a median value of 229.22

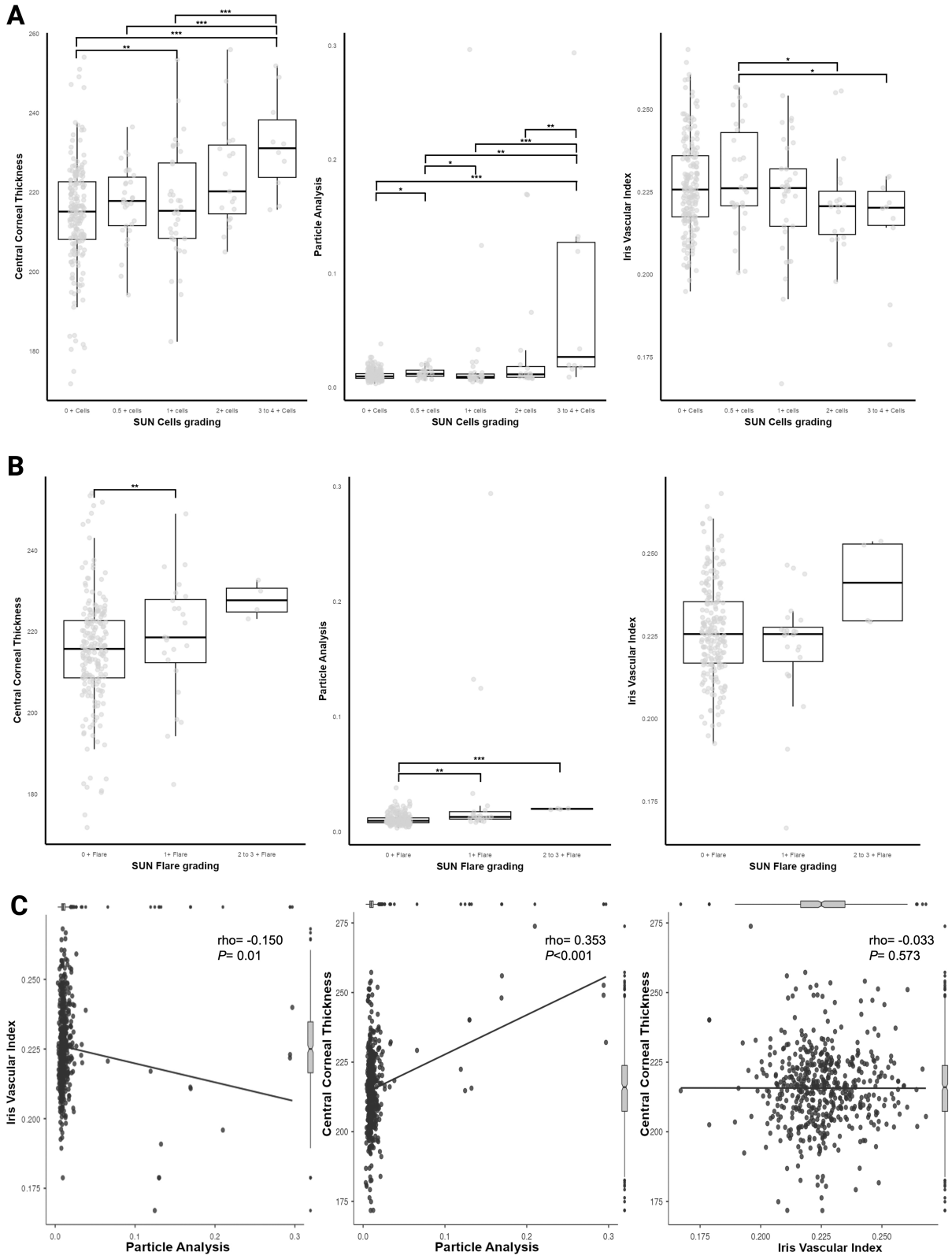

Figure 3. Analysis by cell grading and flare grading, and correlation between measurements. Results of the tool's analysis based on one-way analysis of variance or Kruskal–Wallis tests and post hoc tests adjusted by Holm's test for the comparison of numerical variables, with the selection of the test depending on the data distribution. (**A**) Results of CCT, ACPI, and IVI for patients with uveitis, divided by different grades of AC inflammation based on the SUN classification.[10] (**B**) Results based on the degree of flare in the AC, also according to the SUN classification. (**C**) Correlation between all measurements, with all correlations performed using Spearman's test owing to the data distribution. Significant differences are highlighted with asterisks (*$P < 0.05$, **$P < 0.01$, ***$P < 0.001$).

pixels (95% confidence interval [CI], 208.76–230.04). The ACPI displayed similar robustness, with an AUC of 0.74 and a cutoff range from 0.01185 to 0.01926. Conversely, IVI's utility was limited in this scenario, evidenced by a lower AUC of 0.40 (more details on the performance of all see Figs. 4A and B, and for cut of points in Table 3).

In cases involving 0.5–1+ cells vs. no cells, CCT showed moderate diagnostic effectiveness with an AUC of 0.61 and a cutoff of 208.12 pixels (95% CI, 205.08–

Table 2. Linear Regression for Cell Grading

R	R^2	F	*P* Value
0.481	0.232	28.2	<0.001
Predictor	β	**SD**	***P* value**
Intercept	−0.38565	0.90478	0.67
CCT	0.0096	0.0031	0.002
ACPI	7.62253	1.2033	<0.001
IVI	−6.18205	2.74616	0.025

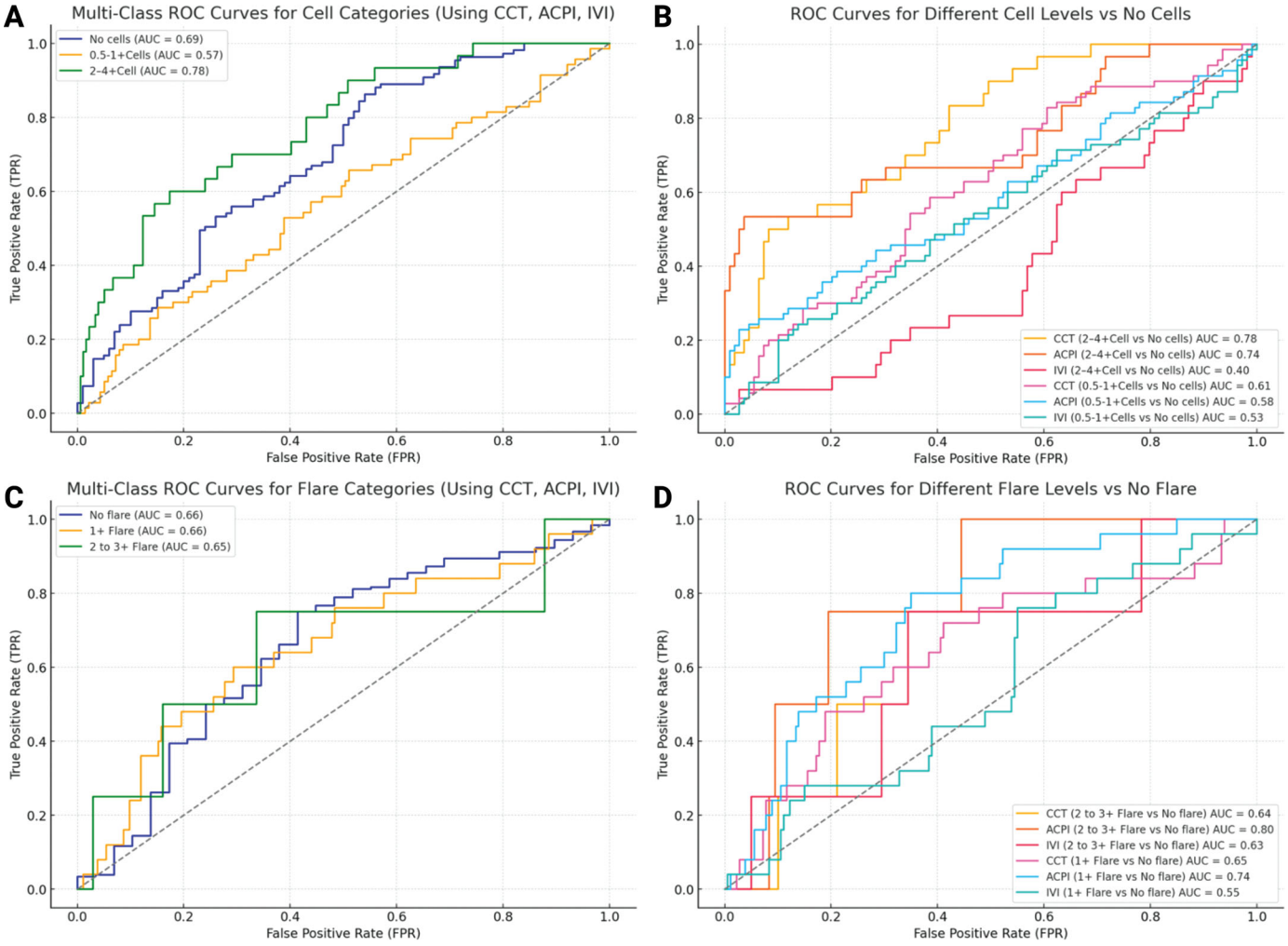

Figure 4. Receiver operating characteristic curves demonstrating the diagnostic performance of CCT, ACPI, and IVI. (**A**) Multiclass receiver operating characteristic curves for cell categories. Receiver operating characteristic curves for different levels of cell presence using CCT, ACPI, and IVI as diagnostic tools. *Blue curve*: No cells (AUC = 0.69); *Orange curve*: 0.5–1+ cells (AUC = 0.57); *Green curve*: 2–4+ cells (AUC = 0.78). (**B**) Receiver operating characteristic curves for different cell levels vs no cells. Performance of CCT, ACPI, and IVI in distinguishing varying levels of cell presence from no cells. *Red curve*: CCT for 2–4+ cells vs no cells (AUC = 0.78); *Orange curve*: ACPI for 2–4+ cells vs no cells (AUC = 0.74); *Blue curve*: IVI for 2–4+ cells vs no cells (AUC = 0.40); *Pink curve*: CCT for 0.5–1+ cells vs no cells (AUC = 0.61); *Turquoise curve*: ACPI for 0.5–1+ cells vs no cells (AUC = 0.58); *Purple curve*: IVI for 0.5–1+ cells vs no cells (AUC = 0.53). (**C**) Multiclass receiver operating characteristic curves for flare categories. Receiver operating characteristic curves for different flare levels using CCT, ACPI, and IVI. *Blue curve*: No flare (AUC = 0.66); *Orange curve*: 1+ flare (AUC = 0.66); *Green curve*: 2 to 3+ flare (AUC = 0.65). (**D**) Receiver operating characteristic curves for different flare levels vs no flare. Diagnostic utility of CCT, ACPI, and IVI in identifying different levels of flare in comparison to no flare. *Red curve*: CCT for 2 to 3+ flare vs no flare (AUC = 0.64); *Orange curve*: ACPI for 2 to 3+ flare vs no flare (AUC = 0.80); *Blue curve*: IVI for 2 to 3+ flare vs no flare (AUC = 0.63); *Pink curve*: CCT for 1+ flare vs no flare (AUC = 0.65); *Turquoise curve*: ACPI for 1+ flare vs no flare (AUC = 0.74); *Purple curve*: IVI for 1+ flare vs no flare (AUC = 0.55).

Table 3. Diagnostic Performance of Ocular Markers in Detecting Flare and Cell Levels

Condition	Marker	AUC	Cutoff Value	95% CI
2 to 3+ Flare vs. No flare	CCT	0.64	219.51	205.08–232.70
	ACPI	0.8	0.0133	0.0106–0.0202
	IVI	0.63	0.2277	0.2130–0.2537
1+ Flare vs. no flare	CCT	0.65	217.55	214.76–227.87
	ACPI	0.74	0.0114	0.0096–0.0155
	IVI	0.55	0.2218	0.2099–0.2440
2 to 4+ Cell vs. no cells	CCT	0.78	229.22	208.76–230.04
	ACPI	0.74	0.015	0.01185–0.01926
	IVI	0.4	0.255	0.1788–1.2605
0.5 to 1+ Cells vs. No cells	CCT	0.61	208.12	205.08–225.66
	ACPI	0.58	0.17	0.00827–0.01984
	IVI	0.53	0.239	0.2205–0.2445

Detailed summary of the receiver operating characteristic analysis for various ocular markers used to distinguish between different levels of flare and cell presence in ocular studies. Each marker's effectiveness is quantified by the AUC, with optimal cutoff values and CIs provided to assist in clinical decision-making.

225.66). ACPI's performance, with an AUC of 0.58 and a wide cutoff range of 0.17 (95% CI, 0.00827–0.01984), and IVI, with an AUC of 0.53 and a cutoff of 0.239 (95% CI, 0.2205–0.2445). (More details on the performance of all see Figs. 4A and B, and for cut of points in Table 3).

Flare-Grading Inflammation Detection

In the context of more pronounced inflammation, distinguishing 2 to 3+ flare from no flare, CCT demonstrated a moderate ability to discriminate, with an AUC of 0.64 and an optimal cutoff at 219.51 (95% CI, 205.08–232.70). The ACPI was notably more effective, recording an AUC of 0.80 and a precise cutoff of 0.0133 (95% CI, 0.0106–0.0202). IVI, with an AUC of 0.63 and a cutoff of 0.2277 (95% CI, 0.2130–0.2537. (More details on the performance of all see Figs. 4C and D, and for cut of points in Table 3.)

For less severe flare, 1+ flare vs. no flare, CCT had an AUC of 0.65, with a cutoff of 217.55 pixels (95% CI, 214.76–227.87). The ACPI achieved an AUC of 0.74 using a cutoff of 0.0114 (95% CI, 0.0096–0.0155). However, IVI seemed to be less effective in milder flare scenarios, with an AUC of 0.55 and a cutoff of 0.2218 (95% CI, 0.2099–0.2440) (for more details, see Figs. 4C and D, and for cut of points in Table 3).

Discussion

Our study evaluated 180 participants, including a significant proportion with uveitis (71.7%), and provided comprehensive insights into the demographic distributions and clinical manifestations associated with the condition. Significant distinctions in CCT and ACPI between patients with uveitis, their contralateral eyes, and control groups were identified, with CCT notably reduced in controls. This analysis extended to variations by uveitis etiology and location, revealing specific patterns in CCT, ACPI, and IVI, offering new understandings into their diagnostic usefulness across different clinical contexts.

Significant findings include CCT's sensitivity to changes in cell grades within the AC, highlighting its potential as a reliable marker in the clinical grading of uveitis. Additionally, the consistent performance of CCT and ACPI under various flare and cell conditions was supported quantitatively by AUC values, reinforcing their roles in precise clinical assessment.

The longitudinal component of the study underscored the stability of CCT and ACPI measurements over 6 months, providing essential validation of these metrics' repeatability and reliability in ongoing clinical settings. These results collectively advance our understanding of ocular inflammatory processes and enhance the diagnostic precision for uveitis, potentially influencing future therapeutic strategies and clinical assessments.

Uveitis is a challenging condition that significantly affects patients and poses considerable challenges for clinicians. If not addressed promptly, uveitis can lead to potentially severe complications, including blindness.[14] Recent research has focused on developing accessible biomarkers, particularly those that measure disease activity objectively.[15–17] These measures are crucial for clinical trials and patient monitoring and could potentially decrease health care costs.[15]

Previous studies addressing this issue have used semiautomated and automated models, as well as neural convolution networks to identify and categorize inflammation in the AC.[15] However, these studies primarily focused on AC cells and flare, neglecting other ocular structures in the AC. It is important to recognize that inflammatory states affect not only the contents of the AC, but also the structures that constitute its borders, such as the cornea and iris.[2]

Our purpose-built, fully automated image analysis algorithm offers a comprehensive view of structural changes in the anterior segment by analyzing not just the contents of the AC but also components that constitute its borders (i.e., cornea, iris) and more objectively grading AC inflammation.

The clinical implications and longitudinal findings show that the CCT's sensitivity to changes in cell grades within the AC highlights its reliability as a clinical marker for grading uveitis. The robust performance of CCT and ACPI under various flare and cell conditions, supported quantitatively by AUC values, reinforces their roles in precise clinical assessments. The longitudinal component of our study emphasized the stability of CCT and ACPI measurements over 6 months, underscoring their repeatability and reliability in clinical settings.

The performance and validation of the model show the capability of fully automated image analysis algorithm to offer a comprehensive view of structural changes in the anterior segment, analyzing not just the contents of the AC, but also the surrounding structures such as the cornea and iris, which are critical for a more objective grading of AC inflammation.

In the context of performance, distinguishing 2 to 3+ flare from no flare, CCT demonstrated moderate discriminative ability (AUC = 0.64) with an optimal cutoff at 219.51 pixels (95% CI, 205.08–232.70 pixels). ACPI showed superior diagnostic accuracy (AUC = 0.80) with a precise cutoff of 0.0133 (95% CI, 0.0106–0.0202), and IVI displayed an AUC of 0.63, highlighting varied effectiveness across different inflammatory conditions (Fig. 4 and Table 3). These findings align with previous reports that evaluate AI tools in AS-OCT cell grading where the highest performance are seen in levels of inflammation and low performance in low grades of inflmmation.[18] Future studies must assess if there is a need to improve data acquisition or if it is the resolution that should improve these results and also if it is better to analyze all the six B-scans or if one B-scan is enough.

Similar to previous developments in AS-OCT, our tool shows statistically significant differences between healthy eyes, contralateral eyes of uveitis patients, and uveitis eyes using the ACPI.[15] Interestingly, we observed that differences occur not only in the ACPI, but also in CCT, aligning with recent systematic reviews and meta-analyses indicating that CCT and endothelial changes might be markers of ocular inflammation, distinguishing disease activity.[19] These findings could be explained by mechanisms that alter the function of corneal endothelial proton pumps, affecting aqueous humor dynamics, and causing subclinical corneal edema, similar to our results. It is also noteworthy that the contralateral eyes showed significantly higher CCT and ACPI, suggesting that ocular inflammation might not be limited to one eye in clinically unilateral uveitis, but rather a subclinical systemic condition affecting both eyes.

Previous studies have not analyzed the iris as a relevant structure for the objective measurement of AC inflammation.[6,20,21] Our results suggest that inflammation and its chronicity affect iris vasculature and stroma. Eyes with more than 1+ cells had significantly reduced IVI, showing an inverse trend to corneal thickness and ACPI, where increased inflammation corresponds to higher CCT and ACPI values. Additionally, our etiological analysis revealed that infectious uveitis patients had thinner corneas but higher IVI, with no significant differences in ACPI. This difference may be because noninfectious and idiopathic uveitis are more chronic and recurrent conditions that generate chronic changes in CCT and in IVI, and also owing to the type of treatment, where more topical steroids are used.[19,22–24] Moreover, our correlation analysis supports these findings. IVI was greater in anterior uveitis than in other types, possibly owing to the primary involvement of the iris in these patients.

Regarding inflammation grading, tools developed in previous studies, like those by Invernizzi et al.,[6] Lu et al.,[25] and Sorkhabi et al.,[26] have shown good performance in assessing AC inflammation compared with manual segmentation and clinical grading. Although our results do not correlate highly with clinical grading in linear regression, our model effectively differentiates cellular inflammation grades in the AC (with the exception of differentiating between 1+ and 2+ AC flare). The lack of high correlation with clinical grading on linear regression may not suggest inaccuracy and lack of predictive power in our model. After all, there are inherent challenges in clinical grading that may limit its reliability and accuracy compared with our model's capabilities, which might account for the weak correlations observed. Indeed, methodologically and statistically, performing correlation analyses between SUN grading and particle analysis results can be problematic owing to the categorical nature of clinical grading variables, leading to potentially misleading significant results in multiple studies[10,27,28] (Fig. 3A).

Animal studies have provided insights into the mechanisms underlying these changes. For instance, studies on experimental autoimmune uveitis in rodents have shown that inflammation may manifest as increased iridal vascular engorgement, adherence of the iris to the lens, and even corneal perforation.[29] These findings support our observations and highlight the potential of IVI as a marker for ocular inflammation.

Further prospective studies are needed to validate our findings using this development, which could be invaluable for objectively assessing AC inflammation and as a potential clinical trial objective outcome. Our study's methodology aims to provide a comprehensive 3D AC grading system, distinguishing it from other studies that may overlook some aspects of ocular inflammation. We recognize limitations in our study, particularly regarding the number of patients with more than 2+ cells, which restricted the tool's ability to show independent differences in patients with 3+ to 4+ cells or 2+ to 3+ flare.

Our study has several limitations. One of the primary challenges is the particle segmentation models used, which may misidentify cornea artifacts as particles owing to their similar appearance. However, this is a tradeoff we made to maximize the model's diagnostic sensitivity for AC particles. Additionally, although most AC cells are leukocytes, our method of particle analysis cannot distinguish between leukocytes, floating pigment, or other types of floaters, which could affect the accuracy of the results. Finally, although the findings from this study are based on single-center data, this limitation is mitigated by the fact that investigator protocol adherence would likely be higher than in a multicenter study; nevertheless, larger-scale studies involving multiple centers are essential to demonstrate the external validity of this quantitative AS-OCT tool in diagnosing uveitis, grading its severity, and evaluating treatment efficacy.

Moreover, this study provides a novel and objective approach to quantifying ocular inflammation using biometric parameters (ACPI, IVI, and CCT). Traditional clinical assessments rely on subjective grading scales, leading to interobserver variability and potential inconsistencies in disease classification. Our findings suggest that these automated, quantitative metrics could improve the precision and reliability of inflammation assessment in clinical practice and research.

Although this study benefits from a 6-month longitudinal analysis, certain limitations should be acknowledged. The image dataset includes both patient-derived and internet-sourced images that, despite stringent selection criteria, may introduce variability in image quality, resolution, and acquisition conditions. Although only images with explicitly stated licenses allowing distribution and modification were included, and public domain images were used in compliance with ethical and legal standards, potential inconsistencies in metadata and clinical annotations remain a consideration.

Moreover, images from patients were collected at different time points (baseline, 1 month, 3 months, 6 months, or 9 months), with a maximum of two time points per patient to avoid over-representation. This approach balances temporal resolution with sample diversity, but may still introduce variability in disease progression tracking. Additionally, the exclusion of certain proprietary datasets and the lack of standardization across publicly sourced images could limit the generalizability of findings.

Despite these limitations, our rigorous preprocessing pipeline, including exclusive assignment of images from the same eye to a single dataset split (training, validation, or testing), data augmentation techniques, and early stopping protocols, enhances the robustness of our model. Future studies should focus on increasing dataset size, incorporating standardized imaging protocols, and ensuring a higher degree of clinical validation across diverse populations.

Conclusions

This study introduces a novel and objective method for quantifying ocular inflammation using ACPI, IVI, and CCT, contrasting with traditional subjective clinical assessments prone to interobserver variability. Our findings reveal that automated, quantitative metrics significantly enhance the precision and reliability of inflammation assessments in both clinical practice and research. The demonstrated reliability over a 6-month period underscores the robustness of these biomarkers, making them invaluable tools for monitoring disease progression and response to treatment over time. This long-term evaluation solidifies the utility of these parameters, setting them apart from other methods that lack longitudinal validation and providing a dependable framework for ongoing clinical application.

Acknowledgments

The authors thank the study participants, the Ng Teng Fong Healthcare Innovation Program, and the National Medical Research Council for their financial support.

Author Contributions: All named authors meet the International Committee of Medical Journal Editors (ICMJE) criteria for authorship for this article, take responsibility for the integrity of the work, and approve this version to be published.

Funding: Research was supported by grants awarded by the National Medical Research Council (NMRC), Ministry of Health, Republic of Singapore grant number NRMC/CSAINV22jul-000, NMRC/CSAINV19nov-0007, and NMRC/CIRG21nov-0023. The funders had no role in study design, data collection and analysis, publication decisions, or manuscript preparation.

Medical Writing/Editorial Assistance: No medical writing or editorial assistance was employed in the preparation of this manuscript. The authors used ChatGPT 4 for spelling and grammar checks of certain sentences. However, all conceptual and intellectual contribution to this work were generated solely by the human authors.

Data and Code Availability: The dataset used and/or analyzed during the current study is available from the corresponding author upon reasonable request.

Disclosure: **C. Cifuentes-González**, None; **L. Gutiérrez-Sinisterra**, None; **W. Rojas-Carabali**, None; **J. Boon**, None; **A. Hudlikar**, None; **X. Wei**, None; **L. Shchurov**, None; **H.H. Oo**, None; **N.C. Loh**, None; **C.S. Shannon**, None; **L.D. Rodríguez-Camelo**, None; **B. Lee** None; **A. de-la-Torre**, None; **R. Agrawal**, None

* CCG and LGS contributed equally and share first authorship.

References

1. Cunningham ETE, Zierhut M. Vision loss in uveitis. *Ocul Immunol Inflamm*. 2021;29:1037–1039, doi:10.1080/09273948.2021.2017152.
2. Whitcup SM, Sen HN. *Whitcup and Nussenblatt's Uveitis*. New York: Elsevier; 2022, doi:10.1016/C2014-0-04249-9.
3. Kempen JH, Ganesh SK, Sangwan VS, Rathinam SR. Interobserver agreement in grading activity and site of inflammation in eyes of patients with uveitis. *Am J Ophthalmol*. 2008;146:813–818.e1, doi:10.1016/j.ajo.2008.06.004.
4. Agarwal A, Ashokkumar D, Jacob S, Agarwal A, Saravanan Y. High-speed optical coherence tomography for imaging anterior chamber inflammatory reaction in uveitis: clinical correlation and grading. *Am J Ophthalmol*. 2009;147:413–416, doi:10.1016/j.ajo.2008.09.024.
5. Sharma S, Lowder CY, Vasanji A, Baynes K, Kaiser PK, Srivastava SK. Automated analysis of anterior chamber inflammation by spectral-domain optical coherence tomography. *Ophthalmology*. 2015;122:1464–1470, doi:10.1016/j.ophtha.2015.02.032.
6. Invernizzi A, Marchi S, Aldigeri R, et al. Objective quantification of anterior chamber inflammation. *Ophthalmology*. 2017;124:1670–1677, doi:10.1016/j.ophtha.2017.05.013.
7. Choi WJ, Pepple KL, Wang RK. Automated three-dimensional cell counting method for grading uveitis of rodent eye in vivo with optical coherence tomography. *J Biophoton*. 2018;11:e201800140, doi:10.1002/jbio.201800140.
8. Von Elm E, Altman DG, Egger M, Pocock SJ, Gøtzsche PC, Vandenbroucke JP. The Strengthening the Reporting of Observational Studies in Epidemiology (STROBE) statement: guidelines for reporting observational studies. *J Clin Epidemiol*. 2008;61:344–349, doi:10.1016/j.jclinepi.2007.11.008.
9. Klement W, El Emam K. Consolidated reporting guidelines for prognostic and diagnostic machine learning modeling studies: development and validation. *J Med Internet Res*. 2023;25:e48763, doi:10.2196/48763.
10. Jabs DA, Nussenblatt RB, Rosenbaum JT; Standardization of Uveitis Nomenclature (SUN) Working Group. Standardization of uveitis nomenclature for reporting clinical data. Results of the First International Workshop. *Am J Ophthalmol*. 2005;140:509–516, doi:10.1016/j.ajo.2005.03.057.
11. Liu Z, Hu H, Lin Y, et al. Swin transformer V2: scaling up capacity and resolution. *2022 IEEE/CVF Conference on Computer Vision and Pattern Recognition (CVPR)*, New Orleans, LA, USA, 2022, pp. 11999–12009. Published online April 11, 2022, doi:10.48550/arXiv.2111.09883.
12. Wu Z, Xiong Y, Yu S, Lin D. Unsupervised feature learning via non-parametric instance-level discrimination. arXiv:1805.01978. Published online May 4, 2018, doi:10.48550/arXiv.1805.01978.
13. Asam JS, Polzer M, Tafreshi A, Hirnschall N, Findl O. Anterior Segment OCT. In: Bille JF, ed. *High Resolution Imaging in Microscopy and Ophthalmology*. New York: Springer International Publishing; 2019:285–299, doi:10.1007/978-3-030-16638-0_13.

14. Maccora I, Marrani E, Pagnini I, et al. Challenges and management of childhood noninfectious chronic uveitis. *Expert Rev Clin Immunol*. 2023;19:599–611, doi:10.1080/1744666X.2023.2198210.
15. Maring M, Saraf SS, Blazes M, et al. Grading anterior chamber inflammation with anterior segment optical coherence tomography: an overview. *Ocul Immunol Inflamm*. 2022;30:357–363, doi:10.1080/09273948.2022.2028289.
16. Kessler LJ, Łabuz G, Auffarth GU, Khoramnia R. Biomarkers to predict the success of treatment with the intravitreal 0.19 mg fluocinolone acetonide implant in uveitic macular edema. *Pharmaceutics*. 2022;14:688, doi:10.3390/pharmaceutics14040688.
17. Bansal R, Gupta A. Protein biomarkers in uveitis. *Front Immunol*. 2020;11:610428, doi:10.3389/fimmu.2020.610428.
18. Uthayananthan P, Tanwar N, Rahi JS, Dick AD, Solebo AL. Imaging-based detection of anterior chamber inflammation: a comparative diagnostic accuracy study. *Am J Ophthalmol*. 2025;270:131–139, doi:10.1016/j.ajo.2024.07.018.
19. Mejía-Salgado G, Muñoz-Vargas PT, Cifuentes-González C, et al. Quantitative changes in the corneal endothelium and central corneal thickness during anterior chamber inflammation: a systematic review and meta-analysis. Grzybowski A, ed. *PLoS One*. 2024;19:e0296784, doi:10.1371/journal.pone.0296784.
20. Pillar S, Kadomoto S, Chen K, et al. Automated quantification of anterior chamber cells using swept-source anterior segment optical coherence tomography. *J Ophthal Inflamm Infect*. 2025;15:3, doi:10.1186/s12348-025-00456-y.
21. Pichi F, Neri P. Overview on automated OCT assessment of anterior chamber cells in uveitis. *Int Ophthalmol*. 2024;44:344, doi:10.1007/s10792-024-03273-9.
22. Ono T, Iwasaki T, Yukawa C, et al. Effect of topical steroid instillation on central corneal thickness in eyes with bullous keratopathy. *Jpn J Ophthalmol*. 2019;63:229–233, doi:10.1007/s10384-019-00658-7.
23. Borrego-Sanz L, Morales-Fernández L, Saénz-Francés San Baldomero F, et al. Corneal biomechanics in non-infectious uveitis measured by Corvis ST: a pilot study. *Ocul Immunol Inflamm*. 2023;31:1765–1771, doi:10.1080/09273948.2022.2108462.
24. Valavil PK. Reduced central corneal thickness associated with long term treatment with topical steroids. *Invest Ophthalmol Vis Sci*. 2006;47:5612.
25. Lu M, Wang X, Lei L, et al. Quantitative analysis of anterior chamber inflammation using the novel CASIA2 optical coherence tomography. *Am J Ophthalmol*. 2020;216:59–68, doi:10.1016/j.ajo.2020.03.032.
26. Sorkhabi MA, Potapenko IO, Ilginis T, Alberti M, Cabrerizo J. Assessment of anterior uveitis through anterior-segment optical coherence tomography and artificial intelligence-based image analyses. *Transl Vis Sci Technol*. 2022;11:7, doi:10.1167/tvst.11.4.7.
27. Makin TR, Orban De Xivry JJ. Ten common statistical mistakes to watch out for when writing or reviewing a manuscript. *eLife*. 2019;8:e48175, doi:10.7554/eLife.48175.
28. Aggarwal R, Ranganathan P. Common pitfalls in statistical analysis: the use of correlation techniques. *Perspect Clin Res*. 2016;7:187, doi:10.4103/2229-3485.192046.
29. Bowers CE, Calder VL, Greenwood J, Eskandarpour M. Experimental autoimmune uveitis: an intraocular inflammatory mouse model. *J Vis Exp*. 2022;12(179):61832, doi:10.3791/61832.